

Materials Design Rules for Multivalent Ion Mobility in Intercalation Structures

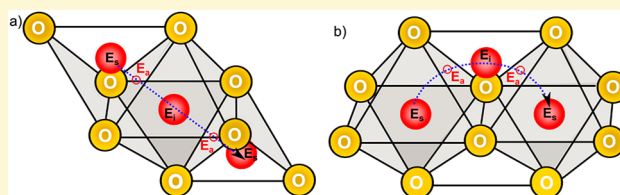
Ziqin Rong,[†] Rahul Malik,[†] Pieremanuele Canepa,[†] Gopalakrishnan Sai Gautam,[†] Miao Liu,[‡] Anubhav Jain,[‡] Kristin Persson,[‡] and Gerbrand Ceder^{*,†}

[†]Department of Materials Science and Engineering, Massachusetts Institute of Technology, Cambridge, Massachusetts 02139, United States

[‡]Environmental Energy Technologies Division, Lawrence Berkeley National Laboratory, Berkeley, California 94720, United States

S Supporting Information

ABSTRACT: The diffusion of ions in solid materials plays an important role in many aspects of materials science such as the geological evolution of minerals, materials synthesis, and in device performance across several technologies. For example, the realization of multivalent (MV) batteries, which offer a realistic route to superseding the electrochemical performance of Li-ion batteries, hinges on the discovery of host materials that possess adequate mobility of the MV intercalant to support reasonable charge and discharge times. This has proven especially challenging, motivating the current investigation of ion mobility (Li^+ , Mg^{2+} , Zn^{2+} , Ca^{2+} , and Al^{3+}) in spinel Mn_2O_4 , olivine FePO_4 , layered NiO_2 , and orthorhombic $\delta\text{-V}_2\text{O}_5$. In this study, we not only quantitatively assess these structures as candidate cathode materials, but also isolate the chemical and structural descriptors that govern MV diffusion. Our finding that matching the intercalant site preference to the diffusion path topology of the host structure controls mobility more than any other factor leads to practical and implementable guidelines to find fast-diffusing MV ion conductors.



1. INTRODUCTION

The energy density requirements of next-generation mobile electronics, electrified vehicles, and renewable energy storage are rapidly outpacing the limit of what is theoretically possible with traditional intercalation-based Li-ion batteries, the current and longstanding industry workhorse.^{1,2} While many new approaches can potentially offer benefits in terms of cost, safety, and specific energy,^{1,3} there are very few options for high energy density (e.g., by volume), which is a critical performance metric in many applications. One promising strategy is to go to a multivalent (MV) chemistry by pairing a MV metal anode (such as Mg, for instance) with a cathode that can reversibly store those MV ions.⁴ Such a cell may be able to achieve energy density well over 1000 Wh/L due to the high volumetric capacity of metal anodes (3830 Ah/L and 8040 Ah/L for Mg and Al, respectively, compared to ~ 700 Ah/L for Li in C) and the high capacity that may be achieved with MV insertion cathodes.² However, the challenges of realizing such a MV battery chemistry are many and complex in nature, which highlight the importance of acquiring fundamental knowledge early on to identify the research directions that are most likely to bear fruit.

The challenges for MV anodes and electrolytes have been well documented,⁵ and in this paper, we focus on understanding and charting the challenge posed by creating cathode host structures with sufficient MV cation mobility required for reversible intercalation at reasonable rates. Indeed, the expectation is that the higher charge of MV cations will

polarize the host environment, thereby reducing mobility and rate capability of MV chemistries. While for Li^+ intercalation both extensive experimental^{6–8} and theoretical^{9–14} Li mobility data are readily available, the lack of reliable electrochemical MV test vehicles^{5,15} and limited exploration of MV chemistries and host structures^{16,17} have made it difficult to understand what controls MV ion mobility. Note that reasonable diffusivity is a required condition for cathode materials but does not guarantee the absence of other potential rate-limiting factors (such as phase transformation or electronic conductivity). Therefore, the objective of this work is to chart the mobility of MV cations in oxide hosts, establish useful guidelines to identify high mobility cathodes, and as such get a better perspective on the feasibility of intercalation-based rechargeable batteries with very high energy density.

In such complex situations, ab initio computing has advantages, as it can isolate distinct physical phenomena and quantitatively assess their thermodynamics and kinetics, which facilitates the identification of the specific structural and chemical features that determine materials properties. Driven by the important role of cation diffusion in geological processes and several technological applications in addition to batteries, phenomenological^{18,19} and empirical^{20–23} models have been developed highlighting factors such as crystal porosity or crystal

Received: June 19, 2015

Revised: August 5, 2015

Published: August 5, 2015

“openness”, electrostatic site energy, and ionic radius of the diffusing species. In this work, we take a significant step forward by harnessing the quantitative accuracy afforded by density functional theory (DFT) nudged elastic band (NEB) simulations^{44–46} to gain deeper insights and arrive at a simple, quantitative recipe for screening compounds and structures. While the NEB method has been applied successfully to address Li diffusion in a multitude of cathode materials providing notable scientific insights,^{47–52} in this study, we extend NEB predictive capabilities to explore the unpaved territory of MV ion migration in selected cathode materials.

In detail, we investigate the migration of MV ions (Mg^{2+} , Zn^{2+} , Ca^{2+} , and Al^{3+}) in four well-known Li-ion intercalation host structures: spinel Mn_2O_4 , olivine FePO_4 , layered NiO_2 , and orthorhombic $\delta\text{-V}_2\text{O}_5$. We also have investigated the thermodynamic properties (voltages and specific capacities) of these materials, which are charted in the [Supporting Information](#). Variants of the first three chemistries have proven to be commercially viable as active cathode materials in Li-ion batteries, and spinel Mn_2O_4 as well as orthorhombic $\delta\text{-V}_2\text{O}_5$ is among the few insertion chemistries known to reversibly intercalate MV ions (along with Chevrel Mo_6S_8 and layered MoO_3).^{4,24–26,43} Moreover, we focus not only on evaluating the suitability of these candidate MV cathode materials on the basis of mobility considerations, but also on identifying the general structural and chemical descriptors that will allow for new MV ion conducting cathode materials to be identified. We find that while the mobility of MV ions is consistently lower than Li^+ , the barrier of different +2 ions depends very strongly on the structure such that the optimal structure for each intercalating ion is different. Indeed, our findings indicate that a structure that has reasonable mobility for one divalent ion may be terrible for another divalent ion. However, clear design guidelines can be established by pairing the diffusion topology of a structure with the site preference of each intercalant.

2. RESULTS AND DISCUSSION

First-principles migration energies are computed using DFT with NEB^{27,28} method with additional computational details provided in the [Supporting Information](#). The migration energies along the diffusion paths in the charged state are shown as solid lines in [Figure 1](#) for (a) spinel Mn_2O_4 , (b) olivine FePO_4 , and (c) layered NiO_2 , with a summary of the migration barriers E_m (e.g., the maximum energy along the path) shown as solid bars in [Figure 1](#), panel d. Note that in these plots, the energies of the intercalation sites (beginning and end points of the path) have been arbitrarily set to zero and the path length normalized to 100% in the x -axis. For adequate battery operation, we quantitatively estimate that E_m can be at most ~ 525 meV when using a micron-sized particle and ~ 650 meV in a nanosized particle. Additional details on how this threshold is estimated are provided in the [Supporting Information](#).

As expected, the Li migration barriers are low, either well below or just above the ~ 525 meV threshold in good agreement with experimentally observed reversible Li intercalation and previous theoretical computations.^{11,12,29,30} MV ion diffusion is categorically poorer than Li^+ diffusion in the same structure, and the Al^{3+} barriers (when able to be converged, as explained further in the [Supporting Information](#)) are higher than all the +2 ions, which in turn exhibit higher barriers than Li^+ . In fact, the Al^{3+} barriers are so high that it is reasonable to conclude that bulk Al^{3+} intercalation into a close-

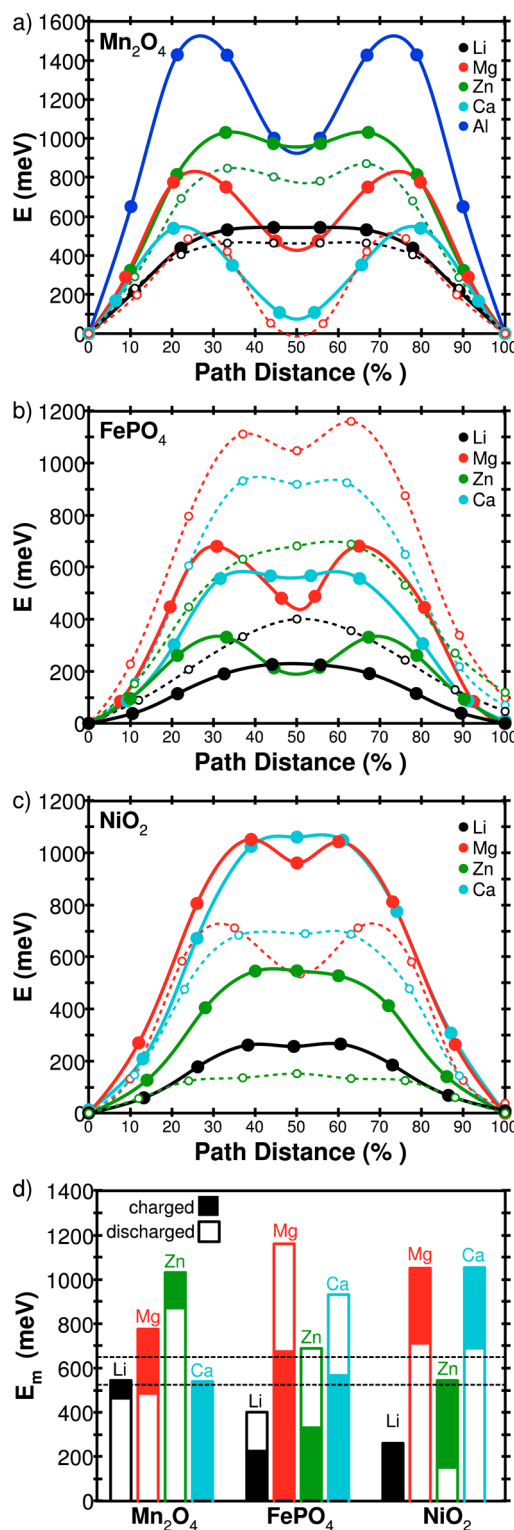


Figure 1. First-principles (NEB) results for Li^+ and MV (Mg^{2+} , Zn^{2+} , Ca^{2+} , and Al^{3+}) migration energies E_m in the (a) spinel Mn_2O_4 , (b) olivine FePO_4 , and (c) NiO_2 structures, in the deintercalated/charged limit (solid lines), and the intercalated/discharged limit (dashed lines), with (d) a summary of migration barriers E_m compared to the prescribed ~ 525 – 650 meV threshold (dashed).

packed oxygen lattice may not be possible at room temperature. The divalent ions (Mg^{2+} , Zn^{2+} , and Ca^{2+}), although noticeably more difficult to intercalate than Li^+ , can be below or near the

~ 525 – 650 meV threshold: Zn^{2+} in FePO_4 and NiO_2 , Mg^{2+} in FePO_4 , or similarly Ca^{2+} in Mn_2O_4 and FePO_4 .

As previously demonstrated in a variety of oxide spinels by Liu et al.,³⁵ the transition metal chemistry does not significantly affect the MV cation diffusion path and respective barriers. We will demonstrate that the general features of the migration energies shown in Figure 1, panels a–c can be rationalized by considering the changing anion coordination environment along the diffusion path. In the close-packed oxygen structures of our model compounds (face-centered cubic *fcc* for spinel and layered, and hexagonal close-packed *hcp* for olivine), the tetrahedral (*tet*) and octahedral (*oct*) interstitial sites share a face. Direct migration between equivalent sites (either *oct* to *oct* or *tet* to *tet*) is usually very high in energy as it requires the ion to pass through a narrow O–O bond,¹⁰ which is also reflected in our result for hop through the oxygen dumbbell in layered NiO_2 shown in Figure S1 in the Supporting Information. Rather, the lower energy path typically crosses through a shared face between *tet* and *oct* sites leading to diffusion topologies that are either *tet* \rightarrow *oct* \rightarrow *tet* (shown in Figure 2a) or *oct* \rightarrow *tet* \rightarrow *oct* (shown in Figure 2b) depending on which insertion site is stable. As an example, the spinel diffusion topology is shown in detail in Figure 2, panel a: the intercalating ion initially resides in the stable tetrahedral *tet* site (with energy E_s), then migrates

through a three-coordinated oxygen face (with energy E_a) shared with the adjacent intermediate octahedral *oct* site (with energy E_i), and finally follows a symmetric path to the next equivalent stable site. In the olivine and layered structures, diffusion proceeds in a similar fashion but between stable octahedral sites through an intermediate tetrahedral site (shown in Figure 2b). Revisiting Figure 1, panels a–c, the local minima are seen to correspond either to the stable or intermediate sites, and maxima either to the three-coordinated or intermediate sites.

Since the *tet* and *oct* sites are always part of the ion migration path, the absolute value of their energy difference $|E_i - E_s|$ shown in Figure 2, panel c is then a lower bound on the migration barrier E_m . In these cases, the energy along the migration path assumes a single “plateau”-type shape, as can be seen in Figure 1.¹⁰

Consequently, the site energy difference (solid bars) can be used as a criterion for mobility screening and in some cases is even identical (e.g., Li^+ in Mn_2O_4 and FePO_4 , Ca^{2+} in NiO_2) or nearly identical (e.g., Li^+ in NiO_2 , Zn^{2+} in Mn_2O_4 , and NiO_2 , and Ca^{2+} in FePO_4) to the migration barrier (hollow bars). The energy differences obtained from our DFT calculations (Figure 2c) correlate well with the known site preference of the intercalated species. In the crystallography and mineralogy literature, the anion coordination environments of several different cations have been exhaustively catalogued: Li^+ and Zn^{2+} are most often found in four-, Mg^{2+} in six-, and Ca^{2+} in eight-coordination.^{31,32} Furthermore, in their systematic study of inverse and normal spinels, Burdett et al. observed the consistent trend that the tetrahedral site preference decreases in order of Li, Zn, Mg, and Ca.^{33,34} Clearly, the combined knowledge of the diffusion topology and preferred coordination environment of the diffusing species now allows us to explain the variation of the barriers in Figure 1. For example, Zn^{2+} has a very high migration barrier in the spinel structure, as its stable insertion site is also its preferred coordination (tetrahedral). Similarly, Mg^{2+} has high migration barriers in both the layered and olivine structures, where the stable insertion site is six-coordinated.

Ca^{2+} prefers to be eight-coordinated and is especially penalized when migrating through a site with significantly lower coordination, explaining the high migration barriers in both layered NiO_2 and olivine FePO_4 , which require migration through an intermediate tetrahedral site. On the other hand, when the intermediate site is the intercalant’s preferred coordination, the site energy difference is smaller, for instance, Li^+ and Zn^{2+} in olivine and layered compared to spinel, and similarly Mg^{2+} in spinel compared to olivine and layered.

To study the effect of intercalant concentration, we also investigated vacancy diffusion barriers in the fully discharged limit in our test structures (dashed lines and hollow bars in Figure 1). For spinel, we used composition $(\text{M})\text{Mn}_2\text{O}_4$, $(\text{M})_{0.5}\text{FePO}_4$ for olivine, and $(\text{M})\text{NiO}_2$ for layered. Although the migration barriers in the discharged limit may either increase (as seen in olivine FePO_4) or decrease (as seen in both spinel Mn_2O_4 and layered NiO_2), our observations relating migration barrier to site preference continue to hold. In the spinel system, the increasing degree of intercalation further stabilizes the intermediate octahedral site due to the decreased electrostatic interaction with reduced nearby transition metal ions, an effect that has also been observed in the studies of Li diffusion in spinel Co_2O_4 , Ni_2O_4 , and Ti_2O_4 systems.^{29,30,35} When the calculations are able to converge, Ca^{2+} is shown to be

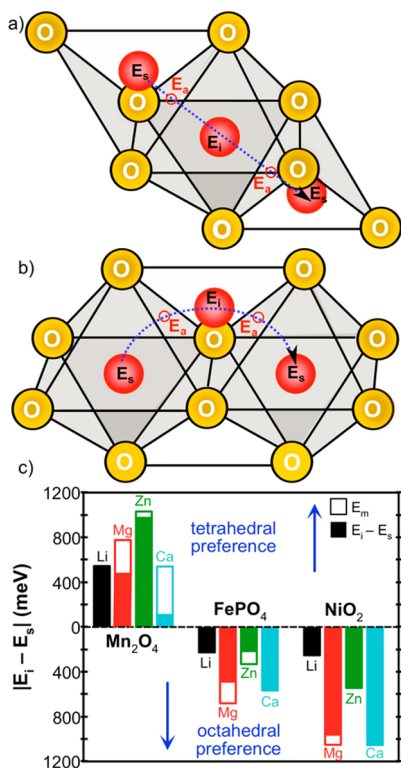


Figure 2. Low-energy ion migration paths in close-packed oxides adopt either (a) *tet* \rightarrow *oct* \rightarrow *tet* or (b) *oct* \rightarrow *tet* \rightarrow *oct* diffusion topologies: beginning in the stable insertion sites (E_s), crossing through a three-coordinated oxygen face (E_a) into the intermediate site (E_i), and finally migrating to the next stable site through a symmetric path. Comparing the (c) site energy difference $|E_i - E_s|$ between *tet* and *oct* sites (solid bars) to the migration barriers E_m (hollow bars) along the diffusion path for Li^+ , Mg^{2+} , Zn^{2+} , and Ca^{2+} in spinel Mn_2O_4 , olivine FePO_4 , and layered NiO_2 reveals the underlying influence of each intercalant’s anion coordination preference on the migration barrier.

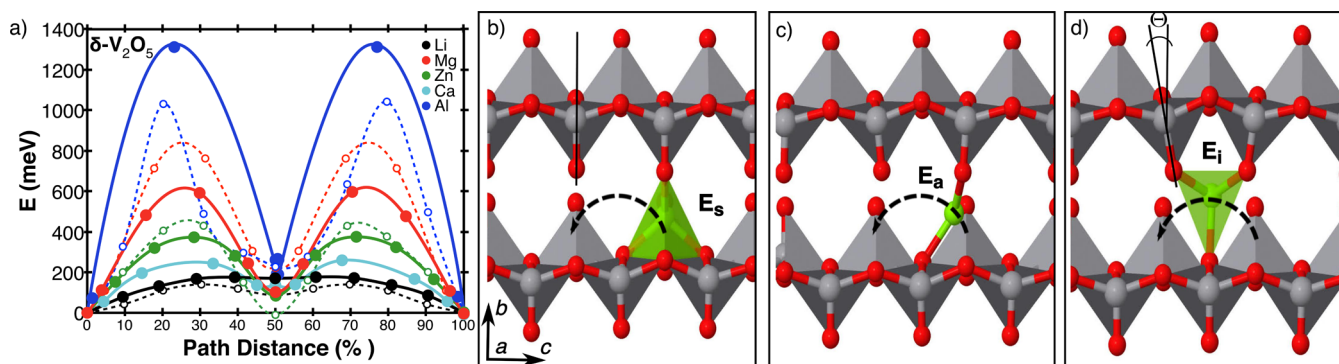


Figure 3. (a) Li and MV migration energies plotted along the diffusion path in δ - V_2O_5 in the empty lattice (solid) and dilute vacancy (dashed) concentration limits as seen for Mg in the (b) stable, (c) activated, (d) and intermediate site.

even more stable in the intermediate octahedral site rather than the tetrahedral site,³⁵ which is a strong indicator of its instability in the normal (tetrahedral occupancy) spinel structure.

For olivine $FePO_4$, we investigated migration in the half-intercalated structure to limit reduction to Fe^{2+} and place the divalent intercalants in a known low-energy ordering of $Li_{0.5}FePO_4$ where the intercalating species occupy alternating octahedral sites oriented along the 1D diffusion direction.³⁶ To arrive at an equivalent stable insertion site now requires migration through two consecutive but symmetrically equivalent *oct-tet-oct* motions, which explains why the migration energies at the end points are larger than zero in Figure 1, panel b. Compared to migration in the empty host, occupation of the intermediate tetrahedral site is further penalized due to the proximity of a nearby intercalated (Li or MV) cation, which pushes the diffusion path away from the tetrahedral site and nearer toward the shared edge between octahedral sites, as seen in Figure 2, panel b. Consequently, the diffusion path begins to resemble direct *oct-oct* migration more so than *oct-tet-oct*, which is reflected in the shift to a “plateau”-type shape of the migration energy and also higher migration barriers, as observed in Figure 1, panel b. In layered NiO_2 , we calculated the migration energy for the low-energy divacancy migration as observed in the $LiCoO_2$ system¹⁰ and found that the MV migration barriers are reduced in the discharged limit as the layer spacing increases, stretching the intermediate tetrahedral site and simultaneously lowering the energy penalty for occupation.^{10,11}

From our quantitative study of cation diffusion, a clear picture emerges on the relation between structure, chemistry, and intercalation mobility. The observed dominance of site energies and coordination preferences would imply that cation mobility is the first order determined by the careful matching of an intercalant’s site preferences and the structure’s topology (for a given anion chemistry) and less so by other factors that have been empirically brought forward such as transition metal chemistry, “openness” of structure, or ionic size. In particular, the fact that we find very different barriers for Zn^{2+} and Mg^{2+} , which have similar ionic size (72–74 pm),³⁷ seems to limit the usefulness of ionic size as factor in estimating mobility. In addition, a recent study on diffusion in spinels found only a small effect on cation mobility from varying the transition metal chemistry.³⁵ Although the particular transition metal chemistry in a structure is not a primary factor, it can influence migration energies through secondary factors such as lattice parameter, site disorder (e.g., Ni in layered compounds³⁸), or subtle changes in electrostatic screening. An example of the latter is

the small difference between late and early transition metal layered compounds.¹¹ The diffusion path is to a large extent controlled by a structure’s topology as ions hop from one site to another through the faces between anion polyhedra, and the energy along the path is controlled by the relative site energies and the preferred coordination of the intercalating ion.

These observations lead us to a two-fold strategy to identify host materials with high MV intercalant mobility: identify structures in which a specific intercalant inserts in a site that does not have its preferred coordination. This makes it more likely that the migration energy will be low as the insertion energy is already “high”, although the lower free energy of insertion comes with a reduction in voltage.³⁹ Our results show several examples of this strategy, Zn^{2+} in olivine $FePO_4$ and layered NiO_2 , Mg^{2+} in spinel, and Ca^{2+} in spinel all fit this description, and all have migration barriers E_m that are either below or very near to the ~ 525 – 650 meV limit. When the opposite occurs, as for Zn^{2+} intercalation in spinel, the migration energy is very high, as seen in Figure 1, panel c. The insertion of a MV ion into a “non-preferred” coordination environment almost certainly guarantees that the discharged structure is thermodynamically metastable rather than thermodynamically stable. We observe this behavior for Ca^{2+} in the discharged spinel structure,³⁵ as well as for Zn^{2+} in layered NiO_2 , in marked contrast to lithium cathodes, which are usually ground states in their discharged (lithiated) state but metastable in their charged state. Our strategy to displace the instability to the discharged state where the cathode is less oxidizing and does not store electrical energy contributes to battery safety. Indeed, in lithium-ion batteries, the maximum oxidation power, largest cathode structure instability, and maximal electrical energy stored in the cell all coincide in the charged state creating a serious thermal runaway and safety problem.⁴⁰ The desire to have the intercalant not in its preferred coordination also calls into question the approach of synthesizing candidate MV cathode materials with the MV ion already present; in this case, it will likely form a structure where its coordination is favorable, making its migration barrier high. Hence, favorable cathodes for MV intercalation should be sought from oxidized host materials that do not contain the intercalant. The materials for which Mg insertion has been established, orthorhombic V_2O_5 , layered MoO_3 , and Chevrel Mo_6S_8 , all display this characteristic identity prototype structures that have low coordination change along the diffusion path, either intrinsic to the structure or by flexibility in the structure. We believe that nanoparticle V_2O_5 in which

slow Mg insertion has been established^{24–26} is an example of such a structure.

The migration energies of Li^+ , Mg^{2+} , Zn^{2+} , Ca^{2+} , and Al^{3+} in the $\delta\text{-V}_2\text{O}_5$ structure are shown in Figure 3, panel a along with the diffusion path illustrated in Figure 3, panels b–d. The δ -phase of V_2O_5 has a pseudolayered structure composed of sheets of edge- and corner-sharing VO_5 square pyramids with the intercalating species sitting in corner-sharing tetrahedral sites, as shown in Figure 3, panel b. Although the intercalating species is situated in what appears to be a tetrahedral environment, there are two additional oxygen atoms nearby. Hence, Mg can be thought of as nominally “4 + 2” coordinated. The diffusion topology is now “4 + 2” – “square pyramid” – “4 + 2” through the three-coordinated shared face (as seen in Figure 3c). More detailed information regarding the V_2O_5 structure can be found in ref 41, and a discussion and comparison to first-principles cation migration energies in the literature^{16,17} are additionally provided in the Supporting Information. Since the coordination change between the stable and intermediate site is smaller than in structures with close-packed anion sublattices (“4 + 2” – 5 – “4 + 2” compared to 4 – 6 – 4), the site energy difference is expected to be smaller, as is indeed observed in Figure 3, panel a, where $E_i - E_s$ is ~ 200 meV or less for all diffusing species considered. Not only are the site energy differences well within the prescribed ~ 525 meV E_m threshold, but also are the barriers for Ca^{2+} and Zn^{2+} in V_2O_5 (also Mg^{2+} is not very high either at ~ 600 meV in the charged state). Indeed, Ca and Mg intercalation has been established in V_2O_5 .²⁴ Careful observation of the V_2O_5 host structure at various stages of MV cation migration shows that the layers ripple (denoted by the angle θ in Figure 3d) according to the structure’s low-energy phonon bending modes,⁴² which facilitate a pseudo four-coordination as the diffusing species migrates through the three-coordinated shared face. Therefore, since there is minimal coordination change along the diffusion path in V_2O_5 , both between the stable (“4 + 2”) site, the intermediate site (square pyramid), and the shared face (pseudo-tetrahedral), the migration barriers are accordingly low as confirmed by the first-principles calculations in this work.

In this paper, we focused on the effect that structural topology has on cation diffusion and did not investigate the effect of anion chemistry though it can substantially influence the migration barrier of intercalants by changing the site preference through size effects and ligand interactions. In addition, the generally better ionic conductivity of sulfides as compared to oxides has been attributed to better screening of the electrostatics by S^{2-} compared to O^{2-} .¹¹ Hence, sulfides may be expected to have better MV-ion mobility than oxides. However, heavier anions will lead to a reduction in specific energy both through their higher weight and through a limit on the voltage they can achieve as the p -states of anions such as S are above the d -states of the oxidized level of the S^{2-} states.

3. CONCLUSIONS

In conclusion, we have charted the migration energy of multiple high-valent intercalation ions in common oxide host materials combining the predicting capabilities of DFT and the NEB approximations. While our results give little hope to use Al^{3+} intercalation in an oxide host for energy storage, the divalent intercalants have close to reasonable migration barriers to enable room temperature intercalation. More importantly, our ability to identify clearly the factors through which structure

governs their migration energy has enabled design guidelines for finding high mobility host materials for divalent cations. We believe that this is an important step forward to realize the full promise of high-energy density storage systems based on MV ions.

■ ASSOCIATED CONTENT

Supporting Information

The Supporting Information is available free of charge on the ACS Publications website at DOI: 10.1021/acs.chemmater.5b02342.

DFT and NEB simulation details (PDF)

■ AUTHOR INFORMATION

Corresponding Author

*Phone: +1 617 253 1581. Fax: +1 617 253 1581. E-mail: gceder@mit.edu.

Author Contributions

Z.R. and R.M. contributed equally to this work.

Notes

The authors declare no competing financial interest.

■ ACKNOWLEDGMENTS

This work was fully supported as part of the Joint Center for Energy Storage Research (JCESR), an Energy Innovation Hub funded by the U.S. Department of Energy, Office of Science, and Basic Energy Sciences. This study was supported by Subcontract No. 3F-31144. We also thank the National Energy Research Scientific Computing Center (NERSC) for providing computing resources. The authors thank the Materials Project (BES DOE Grant No. EDCBEE) for infrastructure and algorithmic support.

■ REFERENCES

- (1) Thackeray, M. M.; Wolverton, C.; Isaacs, E. D. Electrical energy storage for transportation—approaching the limits of, and going beyond, lithium-ion batteries. *Energy Environ. Sci.* **2012**, *5*, 7854–7863.
- (2) Van Noorden, R. The rechargeable revolution: A better battery. *Nature* **2014**, *507*, 26–28.
- (3) Gallagher, K. G.; Goebel, S.; Greszler, T.; Mathias, M.; Oelerich, W.; Eroglu, D.; Srinivasan, V. Quantifying the promise of lithium–air batteries for electric vehicles. *Energy Environ. Sci.* **2014**, *7*, 1555–1563.
- (4) Aurbach, D.; Lu, Z.; Schechter, A.; Gofer, Y.; Gizbar, H.; Turgeman, R.; Cohen, Y.; Moshkovich, M.; Levi, E. Prototype systems for rechargeable magnesium batteries. *Nature* **2000**, *407*, 724–727.
- (5) Muldoon, J.; Bucur, C. B.; Oliver, A. G.; Sugimoto, T.; Matsui, M.; Kim, H. S.; Allred, G. D.; Zajicek, J.; Kotani, Y. Electrolyte roadblocks to a magnesium rechargeable battery. *Energy Environ. Sci.* **2012**, *5*, 5941–5950.
- (6) Park, M.; Zhang, X.; Chung, M.; Less, G. B.; Sastry, A. M. A review of conduction phenomena in Li-ion batteries. *J. Power Sources* **2010**, *195*, 7904–7929.
- (7) Wang, B.; Bates, J. B.; Hart, F. X.; Sales, B. C.; Zuhr, R. A.; Robertson, J. D. Characterization of Thin-Film Rechargeable Lithium Batteries with Lithium Cobalt Oxide Cathodes. *J. Electrochem. Soc.* **1996**, *143*, 3203–3213.
- (8) Amin, R.; Balaya, P.; Maier, J. Anisotropy of Electronic and Ionic Transport in LiFePO_4 Single Crystals. *Electrochem. Solid-State Lett.* **2007**, *10*, A13–A16.
- (9) Van der Ven, A.; Bhattacharya, J.; Belak, A. A. Understanding Li Diffusion in Li-Intercalation Compounds. *Acc. Chem. Res.* **2013**, *46*, 1216–1225.
- (10) Van der Ven, A.; Ceder, G. Lithium Diffusion in Layered Li_xCoO_2 . *Electrochem. Solid-State Lett.* **1999**, *3*, 301–304.

- (11) Kang, K.; Ceder, G. Factors that affect Li mobility in layered lithium transition metal oxides. *Phys. Rev. B: Condens. Matter Mater. Phys.* **2006**, *74*, 094105.
- (12) Morgan, D.; Van der Ven, A.; Ceder, G. Li Conductivity in LiMPO_4 ($M = \text{Mn, Fe, Co, Ni}$) Olivine Materials. *Electrochem. Solid-State Lett.* **2004**, *7*, A30–A32.
- (13) Islam, M.; Driscoll, D.; Fisher, C.; Slater, P. Atomic-Scale Investigation of Defects, Dopants, and Lithium Transport in the LiFePO_4 Olivine-Type Battery Material. *Chem. Mater.* **2005**, *17*, 5085–5092.
- (14) Islam, M. S.; Fisher, C. A. J. Lithium and sodium battery cathode materials: computational insights into voltage, diffusion and nanostructural properties. *Chem. Soc. Rev.* **2014**, *43*, 185.
- (15) Yoo, H. D.; Shterenberg, I.; Gofer, Y.; Gershinsky, G.; Pour, N.; Aurbach, D. Mg rechargeable batteries: an on-going challenge. *Energy Environ. Sci.* **2013**, *6*, 2265.
- (16) Carrasco, J. Role of van der Waals Forces in Thermodynamics and Kinetics of Layered Transition Metal Oxide Electrodes: Alkali and Alkaline-Earth Ion Insertion into V_2O_5 . *J. Phys. Chem. C* **2014**, *118*, 19599–19607.
- (17) Zhou, B.; Shi, H.; Cao, R.; Zhang, X.; Jiang, Z. Theoretical study on the initial stage of a magnesium battery based on a V_2O_5 cathode. *Phys. Chem. Chem. Phys.* **2014**, *16*, 18578.
- (18) Dowty, E. Crystal-chemical factors affecting the mobility of ions in minerals. *Am. Mineral.* **1980**, *65*, 174–182.
- (19) Jost, W. Diffusion and Electrolytic Conduction in Crystals (Ionic Semiconductors). *J. Chem. Phys.* **1933**, *1*, 466–475.
- (20) Fortier, S. M.; Giletti, B. J. An Empirical Model for Predicting Diffusion Coefficients in Silicate Minerals. *Science* **1989**, *245*, 1481–1484.
- (21) Adams, S. Modelling ion conduction pathways by bond valence pseudopotential maps. *Solid State Ionics* **2000**, *136–137*, 1351–1361.
- (22) Adams, S.; Rao, R. P. *Structure and Bonding (Berlin)*; Brown, I. D., Poeppelmeier, K. R., Eds.; Springer: Berlin Heidelberg, 2014; Vol. 158, pp 129–159.
- (23) Brady, J. B.; Cherniak, D. J. Diffusion in Minerals: An Overview of Published Experimental Diffusion Data. *Rev. Mineral. Geochem.* **2010**, *72*, 899–920.
- (24) Amatucci, G. G.; Badway, F.; Singhal, A.; Beaudoin, B.; Skandan, G.; Bowmer, T.; Plitz, I.; Pereira, N.; Chapman, T.; Jaworski, R. Investigation of Yttrium and Polyvalent Ion Intercalation into Nanocrystalline Vanadium Oxide. *J. Electrochem. Soc.* **2001**, *148*, A940.
- (25) Novák, P.; Imhof, R.; Haas, O. Magnesium insertion electrodes for rechargeable nonaqueous batteries — a competitive alternative to lithium? *Electrochim. Acta* **1999**, *45*, 351–367.
- (26) Gershinsky, G.; Yoo, H. D.; Gofer, Y.; Aurbach, D. Electrochemical and Spectroscopic Analysis of Mg^{2+} Intercalation into Thin Film Electrodes of Layered Oxides: V_2O_5 and MoO_3 . *Langmuir* **2013**, *29*, 10964–10972.
- (27) Jonsson, H.; Mills, G.; Jacobsen, K. W. *Classical and Quantum Dynamics in Condensed Phased Simulations* **1998**, 385–404.
- (28) Henkelman, G.; Uberuaga, B. P.; Jónsson, H. A climbing image nudged elastic band method for finding saddle points and minimum energy paths. *J. Chem. Phys.* **2000**, *113*, 9901–9904.
- (29) Bhattacharya, J.; Van der Ven, A. Phase stability and nondilute Li diffusion in spinel $\text{Li}_{1+x}\text{Ti}_2\text{O}_4$. *Phys. Rev. B: Condens. Matter Mater. Phys.* **2010**, *81*, 104304.
- (30) Xu, B.; Meng, S. Factors affecting Li mobility in spinel LiMn_2O_4 —A first-principles study by GGA and GGA+ U methods. *J. Power Sources* **2010**, *195*, 4971–4976.
- (31) Wenger, M.; Armbruster, T. Crystal chemistry of lithium: oxygen coordination and bonding. *Eur. J. Mineral.* **1991**, *3*, 387–400.
- (32) Brown, I. D. What factors determine cation coordination numbers? *Acta Crystallogr., Sect. B: Struct. Sci.* **1988**, *44*, 545–553.
- (33) Burdett, J. K.; Price, G. D.; Price, S. L. Role of the crystal-field theory in determining the structures of spinels. *J. Am. Chem. Soc.* **1982**, *104*, 92–95.
- (34) Navrotsky, A.; Kleppa, O. J. The thermodynamics of cation distributions in simple spinels. *J. Inorg. Nucl. Chem.* **1967**, *29*, 2701–2714.
- (35) Liu, M.; Rong, Z.; Malik, R.; Canepa, P.; Jain, A.; Ceder, G.; Persson, K. A. Spinel compounds as multivalent battery cathodes: a systematic evaluation based on *ab initio* calculations. *Energy Environ. Sci.* **2015**, *8*, 964–974.
- (36) Malik, R.; Zhou, F.; Ceder, G. Kinetics of non-equilibrium lithium incorporation in LiFePO_4 . *Nat. Mater.* **2011**, *10*, 587–590.
- (37) Shannon, R. D. Revised effective ionic radii and systematic studies of interatomic distances in halides and chalcogenides. *Acta Crystallogr., Sect. A: Cryst. Phys., Diffr., Theor. Gen. Crystallogr.* **1976**, *32*, 751–767.
- (38) Kang, K.; Meng, Y. S.; Breger, J.; Grey, C. P.; Ceder, G. Electrodes with High Power and High Capacity for Rechargeable Lithium Batteries. *Science* **2006**, *311*, 977–980.
- (39) Aydinol, M.; Kohan, A.; Ceder, G.; Cho, K.; Joannopoulos, J. *Ab initio* study of lithium intercalation in metal oxides and metal dichalcogenides. *Phys. Rev. B: Condens. Matter Mater. Phys.* **1997**, *56*, 1354–1365.
- (40) Wang, L.; Maxisch, T.; Ceder, G. A First-Principles Approach to Studying the Thermal Stability of Oxide Cathode Materials. *Chem. Mater.* **2007**, *19*, 543–552.
- (41) Chernova, N. A.; Roppolo, M.; Dillon, A. C.; Whittingham, M. S. Layered vanadium and molybdenum oxides: batteries and electrochromics. *J. Mater. Chem.* **2009**, *19*, 2526.
- (42) Popović, Z.; Konstantinović, M.; Gajić, R.; Popov, V.; Isobe, M.; Ueda, Y.; Moshchalkov, V. Phonon dynamics in AV_2O_5 ($A = \text{Na, Ca, Mg, Cs}$) oxides. *Phys. Rev. B: Condens. Matter Mater. Phys.* **2002**, *65*, 184303.
- (43) Kim, C.; Phillips, P. J.; et al. Direct Observation of Reversible Magnesium Ion Intercalation into a Spinel Oxide Host. *Adv. Mater.* **2015**, *27*, 3377–3384.
- (44) Sheppard, D.; Xiao, P.; Chemelewski, W.; Johnson, D. D.; Henkelman, G. A generalized solid-state nudged elastic band method. *J. Chem. Phys.* **2012**, *136*, 074103.
- (45) Sheppard, D.; Henkelman, G. Paths to which the nudged elastic band converges. *J. Comput. Chem.* **2011**, *32*, 1769–1771.
- (46) Sheppard, D.; Terrell, R.; Henkelman, G. Optimization methods for finding minimum energy paths. *J. Chem. Phys.* **2008**, *128*, 134106.
- (47) Ong, S. P.; Chevrier, V. L.; et al. Voltage, stability and diffusion barrier differences between sodium-ion and lithium-ion intercalation materials. *Energy Environ. Sci.* **2011**, *4*, 3680–3688.
- (48) Mo, Y.; Ong, S. P.; Ceder, G. Insights into Diffusion Mechanisms in P2 Layered Oxide Materials by First-Principles Calculations. *Chem. Mater.* **2014**, *26*, 5208–5214.
- (49) Dathar, G. K. P.; Sheppard, D.; Stevenson, K. J.; Henkelman, G. Calculations of Li-Ion Diffusion in Olivine Phosphates. *Chem. Mater.* **2011**, *23*, 4032–4937.
- (50) Song, T.; Cheng, H.; et al. Si/Ge Double-Layered Nanotube Array as a Lithium Ion Battery Anode. *ACS Nano* **2012**, *6*, 303–309.
- (51) Park, K. S.; Xiao, P.; Kim, S. Y.; Dylla, A.; Choi, Y. M.; Henkelman, G.; Stevenson, K. J.; Goodenough, J. B. Enhanced Charge-Transfer Kinetics by Anion Surface Modification of LiFePO_4 . *Chem. Mater.* **2012**, *24*, 3212–3218.
- (52) Tompsett, D. A.; Islam, M. S. Electrochemistry of Hollandite $\alpha\text{-MnO}_2$: Li-Ion and Na-Ion Insertion and Li_2O Incorporation. *Chem. Mater.* **2013**, *25*, 2515–2526.